

Realistic equivalent-photon yields in heavy-ion collisions

Robert N. Cahn

Lawrence Berkeley Laboratory, University of California, Berkeley, California 94720

J. D. Jackson

*Physics Department, University of California at Berkeley, Berkeley, California 94720
and Lawrence Berkeley Laboratory, University of California, Berkeley, California 94720*

(Received 9 March 1990; revised manuscript received 9 August 1990)

Heavy-ion collisions are a potentially prolific source of $\gamma\gamma$ collisions at very-high-energy colliders. However, their utility is limited to events in which the nuclei miss each other. The Weizsäcker-Williams approximation in impact-parameter space is used to evaluate the consequent reduction in photon flux below that obtained by including the effect of the size of the nucleus only through the elastic form factor. The effective luminosity $(\tau/Z^4)d\mathcal{L}/d\tau$ is shown for all relevant circumstances to be a function of the single variable $z = mR/\gamma$, where m is the mass of the created system, R is the nuclear radius, and γ is the center-of-mass-system Lorentz factor of each nucleus. A graph and a simple parametrization are given of $(\tau/L_0)d\mathcal{L}/d\tau$ as a function of z . The effective cross section for production of a Higgs boson with a mass of 100 (150) GeV using Pb-Pb-generated $\gamma\gamma$ collisions is reduced by a factor of roughly 1/2.4 (1/3) at the Superconducting Super Collider and a factor of 1/4.6 (1/7) at the CERN Large Hadron Collider by the exclusion of events in which the nuclei collide.

I. INTRODUCTION

Heavy ions have been considered recently as a potential source for high-energy $\gamma\gamma$ collisions, possibly using the CERN Large Hadron Collider (LHC) or the Superconducting Super Collider (SSC). The advantage of using heavy ions is that the cross sections varies as $Z^4\alpha^4$ rather than just as α^4 . The $\gamma\gamma$ collisions are especially interesting because they would produce the orthodox Higgs boson, provided this particle exists and is not too massive.¹⁻³ A Higgs boson in the mass region between 80 and 125 GeV or so would be most intriguing in this regard since this is above the reach of the CERN e^+e^- collider LEP II and below the domain accessible at the SSC. To attempt to produce the Higgs boson in this way would require operating the proposed LHC or the SSC with heavy ions. The luminosity under such conditions might be of order $10^{28} \text{ cm}^{-2} \text{ s}^{-1}$.⁴ The energy per nucleon at the LHC would be about 3.2 TeV, while at the SSC it would be about 8 TeV.

Some of the difficulties associated with this potential search for the Higgs boson have been examined by Drees *et al.*³ The complexity of the basic nuclear collisions requires that the $\gamma\gamma$ process occur without disruption of the nuclei or even significant overlap of the tails of their nucleon densities. The hadronic production by a single nucleon-nucleon collision (from "halo" overlap) of two jets (approximately 20% $b\bar{b}$) with an invariant mass in the range of the Higgs-boson mass is of the order of 10^6 times the $\gamma\gamma$ production of the Higgs boson. Even if the nuclear "halos" do not overlap, the decay of the Higgs boson into $b\bar{b}$ would have to be identified in the face of a

$b\bar{b}$ background produced directly from $\gamma\gamma$ collisions and a much larger background from $\gamma\gamma$ producing lighter quark pairs. The energy-resolution requirements are daunting. Nonetheless, Drees *et al.* suggested that it might be feasible to search for the Higgs boson at the LHC and SSC using heavy-ion $\gamma\gamma$ collisions.

The calculations in Refs. 1-3 appear not to have imposed the restriction that the nuclei have no significant overlap, thereby overestimating the cross section. Cahn⁵ attempted to correct for nuclear overlap in a simple way by using equivalent-photon spectra with minimum impact parameters $b_{\min} = 2R$ for each ion. This recipe, leading to an overly pessimistic estimate of the cross section, was also used in a preliminary version of the present paper.⁶ Baur⁷ has stated a sensible recipe for obtaining realistic equivalent-photon spectra for nondisruptive collisions of relativistic ions. We employ his recipe here. Since by now there are a large number of essentially equivalent computations of Higgs-boson production (and other processes) in relativistic heavy-ion collisions,⁸⁻¹² some written at least partially in response to Ref. 6, we emphasize here the universal scaling behavior of the effective luminosity for both the simple factorized form and that resulting from Baur's recipe. We present the results graphically and in a readily usable analytic approximation in terms of the scaling variable $z = mR/\gamma$, where m is the mass of the system produced in the two-photon collision, R is the nuclear radius, and γ is the center-of-mass-system (c.m.s.) Lorentz factor of each heavy ion. If s is the square of the c.m.s. energy of the two (equal-mass) ions, $\gamma = \sqrt{s}/2M$, where M is the mass of each ion. The cross section for Higgs-boson production is given as an example.

II. EQUIVALENT PHOTON SPECTRA AND EFFECTIVE LUMINOSITY

In the equivalent-photon approximation, we denote the joint number distribution of the two photons carrying fractions of the total momentum of each nucleus between x_1 and x_1+dx_1 and x_2 and x_2+dx_2 , respectively, as $F(x_1, x_2)dx_1dx_2$. In general, this distribution does not factor into separate spectra for the two nuclei, but it does in some circumstances (if nuclear overlap is ignored or in a simple-minded treatment of the overlap). Initially we assume factorization is valid: $F(x_1, x_2)=f(x_1)f(x_2)$, where for simplicity we assume the nuclei are identical and with identical (and opposite) momenta. Then the effective differential luminosity to produce a system of mass m is

$$\begin{aligned} \frac{d\mathcal{L}}{d\tau} &= \int_{\tau}^1 dx_1 dx_2 f(x_1) f(x_2) \delta(\tau - x_1 x_2) \\ &= \int_{\tau}^1 \frac{dx}{x} f(x) f\left(\frac{\tau}{x}\right), \end{aligned} \quad (1)$$

where $\tau=m^2/s$. For orientation we note that in Pb-Pb collisions in the LHC and SSC the values of s are about 1.7×10^6 and 1.1×10^7 TeV², respectively. For $m \sim 100$ GeV, the τ values are 6×10^{-9} and 10^{-9} , respectively.

There remains only to find $f(x)$. Because enhancement will occur only if the process is coherent, it is natural to include a form factor for the nucleus. A straightforward calculation of f , including the nuclear form factor, gives³

$$f(x) = \frac{Z^2 \alpha}{\pi x} \int_{x^2 M^2}^{\infty} \frac{dQ^2}{Q^2} F(Q^2)^2 \left[1 - \frac{x^2 M^2}{Q^2} \right], \quad (2)$$

where M is the mass of the nucleus. If the source were instead an electron, the form factor would be absent as would the $x^2 M^2/Q^2$ term. Setting the upper limit of integration to s and Z to 1 would give $f \approx (\alpha/\pi x) \ln(s/m_e^2)$, in agreement with the usual Weizsäcker-Williams form

$$f_{WW}(x) = \left[\frac{\alpha}{\pi x} \ln \frac{s}{4m_e^2} \right] \frac{1}{2} [1 + (1-x)^2]. \quad (3)$$

Drees, Ellis, and Zeppenfeld³ (DEZ) approximated the form factor for heavy nuclei by an exponential

$$F(Q^2)^2 = \exp(-Q^2/Q_0^2), \quad (4)$$

with $Q_0 = 55-60$ MeV for Pb. This gives³

$$f_{\text{DEZ}}(x) = \frac{Z^2 \alpha}{\pi x} \left[\left[1 + \frac{x^2 M^2}{Q_0^2} \right] E_1 \left[\frac{x^2 M^2}{Q_0^2} \right] - e^{-x^2 M^2/Q_0^2} \right]. \quad (5)$$

For very small values of x , we have

$$f_{\text{DEZ approx}}(x) = \frac{Z^2 \alpha}{\pi x} \left[\ln \frac{Q_0^2}{(xM)^2} - 1.577 \right]. \quad (6)$$

In an earlier work Papageorgiu used²

$$f_P(x) = \frac{Z^2 \alpha}{\pi x} \ln \frac{1}{(xMR)^2}. \quad (7)$$

To compare these approximations we write

$$f_{\text{DEZ approx}}(x) = \frac{Z^2 \alpha}{\pi x} \left[\ln \frac{1}{(xMR)^2} - 1.577 + \ln Q_0^2 R^2 \right]. \quad (8)$$

For Pb, $\ln Q_0^2 R^2 = 1.40$, if $R = 1.2 A^{1/3}$ fm, and so the DEZ result is just slightly smaller than that of Papageorgiu in the region of very small x . At larger x , however, the DEZ form is larger. In particular, the Papageorgiu distribution vanishes for $x > 1/MR \approx 1.5 \times 10^{-4}$.

The above expressions for $f(x)$ are applicable provided the nuclei are never disrupted in a collision. However, as discussed above, realistic equivalent-photon fluxes must be based on the requirement that the nuclei do not physically collide.

As regards the nuclei, the process is classical, with Coulomb deflection of the nuclei neglected ($\Delta p_{\perp} \sim 1$ GeV/ c for grazing Pb nuclei). The equivalent-photon approximation should be evaluated in impact-parameter space, with the geometry of the situation as shown in Fig. 1. The point P is the two-photon collision point. The equivalent-photon spectra of the two nuclei are to be integrated over in the same manner as the transverse profiles of particle beams to find a collider's luminosity, but excluding nuclear overlap. There is a question of whether the collision point P should lie inside either nucleus. This represents Higgs-boson production in the line of flight of the nuclear interior. We exclude the nuclear interiors because (a) the photon flux is a maximum at the nuclear surface and decreases rapidly inside, and (b) Higgs-boson-nucleus interaction effects may disturb the cleanness of the events. The joint number distribution is therefore given by⁷

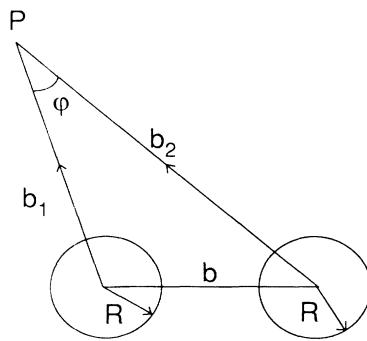


FIG. 1. Geometry of the two-photon process in the transverse plane. The nuclei of radius R are separated by an impact parameter b . The point P at which the two-photon flux is evaluated is displaced by \mathbf{b}_1 and \mathbf{b}_2 from the nuclei. The integral in Eq. (9) is restricted to the region $|\mathbf{b}_1 - \mathbf{b}_2| > 2R$.

$$F(x_1, x_2) = 2\pi \int_R^\infty b_1 db_1 \times \int_R^\infty b_2 db_2 \times \int_0^{2\pi} d\phi \frac{d^2 f}{d^2 b_1}(x_1) \times \frac{d^2 f}{d^2 b_2}(x_2) \theta(b - 2R), \tag{9}$$

where¹³

$$\frac{d^2 f}{d^2 b}(x) = \frac{Z^2 \alpha}{\pi^2 x} \frac{1}{b^2} [(xMb)^2 K_1^2(xMb)] + O\left[\frac{1}{\gamma^2}\right]. \tag{10}$$

It is useful to have the integral of Eq. (10) over all angles and $b > b_{\min}$:

$$f_{cl}(x, b_{\min}) = \frac{2Z^2 \alpha}{\pi x} \left\{ \left[\frac{x}{x_0} \right] K_0 \left[\frac{x}{x_0} \right] K_1 \left[\frac{x}{x_0} \right] - \frac{1}{2} \left[\frac{x}{x_0} \right]^2 \left[K_1^2 \left[\frac{x}{x_0} \right] - K_0^2 \left[\frac{x}{x_0} \right] \right] \right\}, \tag{11}$$

$$\Delta F(x_1, x_2) = 4\pi \int_R^\infty b_1 db_1 \int_{b_>}^{b_1+2R} b_2 db_2 \frac{d^2 f}{d^2 b_1}(x_1) \frac{d^2 f}{d^2 b_2}(x_2) \arccos \left[\frac{b_1^2 + b_2^2 - 4R^2}{2b_1 b_2} \right], \tag{16}$$

with $b_>$ the larger of $b_1 - 2R$ and R . Three comments are in order: (1) The nonfactorizable $\Delta F(x_1, x_2)$ corresponds to the elimination of overlap of the two nuclei; (2) the structure of Eq. (15) and the behavior of $f_{cl}(x)$ with b_{\min} leads us to anticipate that $F(x_1, x_2)$ may be approximated by a factorized form with a somewhat larger nuclear radius, at least as far as the effective luminosity is concerned; (3) as discussed by Baur,⁷ the exclusion of nuclear overlap affects the spectra of the parallel and perpendicular polarization states of the virtual photons differently. Calculations⁸ show the effect to be small. We ignore it here.

The contribution of the first (factorized) term in (15) to the effective luminosity can be written

$$\tau \frac{d\mathcal{L}_1}{d\tau} = \left[\frac{2Z^2 \alpha}{\pi} \right]^2 \int_\tau^1 \frac{dx}{x} \bar{f} \left[\frac{x}{x_0} \right] \bar{f} \left[\frac{\tau}{xx_0} \right], \tag{17}$$

where $\bar{f}(x/x_0)$ is the curly-bracketed expression in Eq. (11). A change of variable leads to

$$\tau \frac{d\mathcal{L}_1}{d\tau} = \left[\frac{2Z^2 \alpha}{\pi} \right]^2 \int_{MR\tau}^{MR} \frac{dy}{y} \bar{f}(y) \bar{f} \left[\frac{z^2}{4y} \right], \tag{18}$$

where $x_0 = 1/b_{\min} M$. For very small argument z ,

$$K_0(z) \rightarrow -\ln(z/2) - \gamma, \tag{12}$$

$$K_1(z) \rightarrow 1/z, \tag{13}$$

and so for small values of x and $b_{\min} = R$, we have

$$f_{cl \text{ approx}}(x, R) = \frac{Z^2 \alpha}{\pi x} \left[\ln \frac{1}{(xMR)^2} - 0.768 \right], \tag{14}$$

a result that is somewhat below those of Drees *et al.* and Papageorgiu. This difference becomes greater as x increases, but there is little point in further comparing the approximations (7), (8), and (14) since they have applicability only in the extremely small- x region.

The expression of real interest is the unfactorizable form (9). It is elementary to show that Eq. (9) can be written

$$F(x_1, x_2) = f_{cl}(x_1, R) f_{cl}(x_2, R) - \Delta F(x_1, x_2), \tag{15}$$

where

where $z = 2MR \sqrt{\tau} = mR/\gamma$. The upper and lower limits of integration are

$$MR = 5.665 A^{4/3}, \quad \tau MR = z^2 / 22.66 A^{4/3}, \tag{19}$$

where we have put $R = 1.2 A^{1/3}$ fm. For $A \geq 200$, $MR \geq .6.6 \times 10^3$ and $\tau MR \lesssim 3.8 \times 10^{-5} z^2$. For heavy ions we see that the upper limit is large compared to unity, and for $z < 10$ the lower limit is small compared to unity. The product $\bar{f}(y) \bar{f}(z^2/4y)$ in the integral (18) vanishes exponentially (times a logarithm) at both limits. Replacing the actual limits in (18) by zero and infinity does not affect the result. Thus the integral is a function only of z for relevant values of A and z . The first term in the effective luminosity can thus be written

$$\tau \frac{d\mathcal{L}_1}{d\tau} = \mathcal{L}_0 \xi_1(z), \tag{20}$$

where \mathcal{L}_0 is chosen for later convenience to be

$$\mathcal{L}_0 = \frac{16Z^4 \alpha^2}{3\pi^2}. \tag{21}$$

The overlap correction to the effective luminosity from $\Delta F(x_1, x_2)$ [Eq. (16)] can be similarly written as

$$\Delta \left[\tau \frac{d\mathcal{L}}{d\tau} \right] = \frac{3}{4\pi} \mathcal{L}_0 \int_{MR\tau}^{MR} \frac{dy}{y} \int_1^\infty \beta_1 d\beta_1 \int_{\beta_>}^{\beta_1+2} \beta_2 d\beta_2 K_1^2(\beta_1 y) K_1^2 \left[\beta_2 \frac{z^2}{4y} \right] \arccos \left[\frac{\beta_1^2 + \beta_2^2 - 4}{2\beta_1 \beta_2} \right], \tag{22}$$

where $\beta_>$ is the larger of $(\beta_1 - 2)$ and 1, and $\beta_1 = b_1/R_1$, $\beta_2 = b_2/R$. With the same behavior of the integrand at the upper and lower limits in y , we can safely extend that interval to $(0, \infty)$. Then the correction (22) also becomes a function of z alone. The final result is that the effective luminosity times τ can be written as

$$\tau \frac{d\mathcal{L}}{d\tau} = \mathcal{L}_0 \xi(z), \quad (23)$$

where Eq. (23) is the difference of Eqs. (18) and (22). Figure 2 shows the result of the computation as a function $z = 2MR\sqrt{\tau} = mR/\gamma$. The quantity plotted is $\xi(z) = (\tau/\mathcal{L}_0)d\mathcal{L}/d\tau$. Also shown in the figure are the results from the factorized form (18) with $b_{\min} = 1.0R$ and $1.2R$, illustrating the fact that the Baur recipe is approximately equivalent to the choice of a slightly larger radius.

If the generic small- x form [encompassing Eqs. (6), (7), and (14)]

$$f_{\text{cl}}(x, R) \simeq \frac{2Z^2\alpha}{\pi x} \ln \left[\frac{\lambda}{xMR} \right] \quad (24)$$

is employed to compute the factorized effective luminosity [Eq. (18)], the result is

$$\lim_{z \ll 1} \frac{\tau d\mathcal{L}}{d\tau} = \mathcal{L}_0 \left[\ln \left[\frac{2\lambda}{z} \right] \right]^3. \quad (25)$$

An explicit fit to the numerical integration displayed graphically in Fig. 2, accurate to 2% or better for $0.05 < z < 5.0$, is

$$\xi(z) = \sum_{j=1}^3 A_j e^{-b_j z}, \quad (26)$$

with $A_1 = 1.909$, $A_2 = 12.35$, $A_3 = 46.28$, $b_1 = 2.566$,

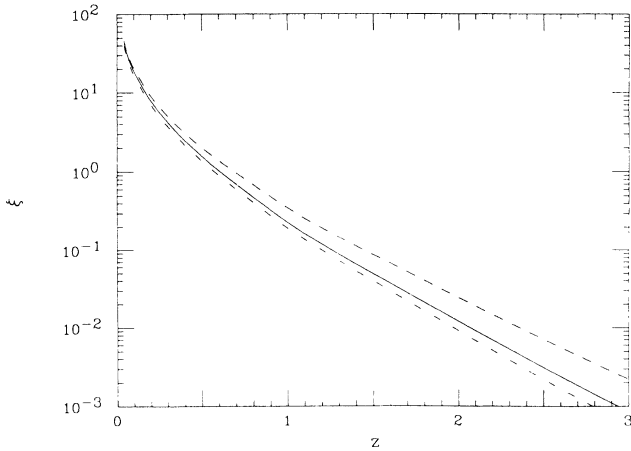


FIG. 2. Dimensionless universal luminosity function $\xi = (\tau/\mathcal{L}_0)d\mathcal{L}/d\tau$ as a function of $z = mR/\gamma$ is shown as the solid curve. The (upper) dashed curve corresponds to the factorized form ξ_1 with $b_{\min} = R$. See Eqs. (17)–(20). The (lower) dot-dashed curve corresponds to the same factorized form, but with $b_{\min} = 1.2R$.

$b_2 = 4.948$, and $b_3 = 15.21$. This parametrization does not reflect the small- z behavior of Eq. (25), but has the advantage of simplicity, useful if integration over z is required in some application. For $z < 0.05$, the expression (25) is adequate, with $2\lambda = 1.234$. This choice of 2λ is equivalent to the choice of $b_{\min} \approx 1.1R$ with the factorized form (18).

III. HIGGS-BOSON PRODUCTION AND OTHER CROSS SECTIONS

As an illustration of the use of the realistic equivalent-photon spectra and effective luminosity shown in Fig. 2, we calculate the cross section for production of a Higgs particle as a function of m_H in nondisruptive collisions of relativistic heavy ions, in particular for Pb-Pb collisions at c.m.s. energies of 3.2 TeV/nucleon (LHC) and 8.0 TeV/nucleon (SSC).

An effective nuclear radius R must be chosen. How much halo interaction and nuclear disruption can be tolerated is an experimental question, but the results are insensitive to the exact choice of R . Electron-scattering data¹⁴ give half-height radii for an assumed Fermi distribution of charge of $c \approx 1.1 A^{1/3}$ fm for heavy nuclei and corresponding equivalent radii for a uniform charge distribution of $R_{\text{equiv}} = (5\langle r^2 \rangle/3)^{1/2} \approx 1.2 A^{1/3}$ fm. The charge thickness parameter in such nuclei is $t \approx 2.3 \pm 0.2$ fm. Since the neutron distribution in heavy nuclei extends one or more femtometers beyond the protons, we take $R \approx 1.2 A^{1/3}$ fm with the belief we are not underestimating the measurable Higgs-boson cross section and may be slightly overestimating it.

In the narrow resonance approximation, the effective cross section for producing the Higgs boson is

$$\sigma_{\text{Higgs via } \gamma\gamma} = \left[\frac{8\pi^2}{m_H^3} \Gamma(H \rightarrow \gamma\gamma) \right] \tau \frac{d\mathcal{L}}{d\tau}, \quad (27)$$

where $\tau = m_H^2/s$, and $\tau d\mathcal{L}/d\tau$ is to be evaluated at the appropriate value of $z = m_H R/\gamma$.

The $\gamma\gamma$ width of a Higgs boson with $m_H \ll m_W$ is given by¹⁵

$$\Gamma(H \rightarrow \gamma\gamma) = \frac{\alpha^2 G_F m_H^3}{128\pi^3 \sqrt{2}} \left| 7 - \frac{4}{3} \sum_f Q_f^2 C_f I \left[\frac{m_f^2}{m_H^2} \right] \right|^2, \quad (28)$$

where C_f is the color factor that is 3 for quarks and 1 for leptons. The function $I(z)$, generally complex, is near 1 for large argument and near 0 for small argument so that only fermions heavy compared to the Higgs bosons are counted. For the domain of interest, we include only the t quark. If the mass of the Higgs boson is not small compared to the mass of the W , the 7 in Eq. (28) is replaced by a factor involving $I(m_W^2/m_H^2)$. An adequate approximation throughout the region of interest ($m_H < 2m_W$) is

$$\Gamma(H \rightarrow \gamma\gamma) = 3 \text{ keV} \left[\frac{m_H}{100 \text{ GeV}} \right]^3. \quad (29)$$

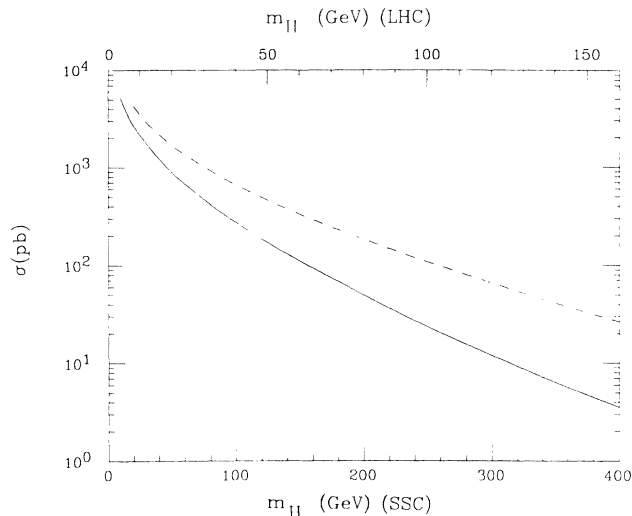


FIG. 3. Cross section for producing a Higgs boson through Pb-Pb-generated photon-photon collisions as a function of the Higgs-boson mass is shown by the solid curve. The lower mass scale is appropriate for the SSC (8 TeV per nucleon), the upper for the LHC (3.2 TeV per nucleon). The dashed curve gives the result using the formula of Ref. 3, our Eq. (5) in Eq. (1). Both curves use the approximation Eq. (29) for $\Gamma(H \rightarrow \gamma\gamma)$.

The factor in large parentheses in Eq. (27) is roughly 90 fb, independent of the Higgs-boson mass.

The $\gamma\text{-}\gamma$ production cross sections in Pb-Pb collisions as functions of Higgs-boson mass using Eq. (23) and the Drees *et al.* expression derived from Eq. (5) are shown in Fig. 3. With the assumption of constancy for the expression in large parentheses in (27), a single curve suffices for LHC and SSC energies (or any other energy or ion) because of the z scaling of $\tau d\mathcal{L}/d\tau$. For convenience, we show separate mass scales for the two accelerators (bottom for SSC, top for LHC). A more accurate evaluation of $\Gamma(H \rightarrow \gamma\gamma)$ would increase both cross sections in the mass range $m_H \sim 2m_W$ (by a factor of about 1.3 at $m_H = 100$ GeV and 3.7 at $m_H = 160$ GeV). This improvement will not affect the relative comparison of the result of Drees *et al.* with our result.

It is apparent from Fig. 3 that requiring that the two nuclei miss each other reduces the cross section for Higgs-boson production through the $\gamma\gamma$ process. For the SSC parameters, the reduction amounts to a factor of 2.4 for $m_H = 100$ GeV and 3.1 for $m_H = 150$ GeV in comparison with the results obtained from the model of Drees *et al.* At the LHC these factors are 4.6 and 7.0, respectively. The cross sections of the solid curve in Fig. 3 [even augmented by a better estimate of $\Gamma(H \rightarrow \gamma\gamma)$] give marginal rates. LHC running 10^7 s per year at a luminosity of 10^{28} $\text{cm}^{-2}\text{s}^{-1}$ with Pb would get three 100-GeV Higgs bosons per year. At the SSC the yield would be 10 times as great—still marginal. In addition to the question of rates, there are great difficulties with backgrounds, mass resolution, and tagging.¹⁶

If there is a mass dependence of the expression in large parentheses in Eq. (27), a single graph with scaled abscissas is not adequate to describe the cross sections for different nuclei and/or energies. Nevertheless, the scaling form of $\xi(z)$ shown in Fig. 2 permits rapid evaluation of two-photon cross sections in nondisruptive collisions of relativistic heavy ions. If the real two-photon cross section for a final state f of invariant mass m is denoted by $\sigma_{\gamma\gamma \rightarrow f}(m^2)$, the Weizsäcker-Williams cross section for producing the same final state per unit interval in m^2 in heavy-ion collisions is

$$\frac{d\sigma_{WW}(m^2)}{dm^2} = \frac{\sigma_{\gamma\gamma \rightarrow f}(m^2)}{m^2} \mathcal{L}_0 \xi(z), \quad (30)$$

where $z = mR/\gamma$. For $\mu^+\mu^-$ and $\tau^+\tau^-$ production, for example, the parametrization (26) together with the QED cross section for $\gamma\gamma \rightarrow l^+l^-$ easily yields results agreeing with the curves of Ref. 8 within a few percent.

ACKNOWLEDGMENTS

This work was supported by the Director, Office of Energy Research, Office of High Energy and Nuclear Physics, Division of High Energy Physics of the U.S. Department of Energy under Contract No. DE-AC03-76SF00098.

¹M. Grabiak *et al.*, GSI Report No. 87-78, 1987 (unpublished); *J. Phys. G* **15**, L25 (1989); G. Soff *et al.*, in *The Nuclear Equation of State, Part B* (NATO Advanced Study Institute Series B: Physics, Vol. 216), proceedings, Peñiscola, Spain, 1989, edited by W. Greiner and H. Stöcker (Plenum, New York, 1989), p. 579.

²E. Papageorgiu, *Phys. Rev. D* **40**, 92 (1989); *Nucl. Phys.* **A498**, 593c (1989). See also Report No. MPI-PAE/PTh 68/89 (unpublished) for an extensive discussion of two-photon processes in heavy-ion collisions.

³M. Drees, J. Ellis, and D. Zeppenfeld, *Phys. Lett. B* **223**, 454 (1989).

⁴M. Drees, presented at XII Warsaw Symposium on Elementary Particle Physics, Kazimierz, Poland, 1989 (unpublished).

⁵R. N. Cahn, in *Proceedings of the XIVth International Symposium on Lepton and Photon Interactions*, Stanford, California, 1989, edited by M. Riordan (World Scientific, Singapore, 1989), p. 60 (see Fig. 14.1 and Sec. 17).

⁶R. N. Cahn and J. D. Jackson, Lawrence Berkeley Laboratory Report No. LBL-28592, 1990 (unpublished).

⁷G. Baur, in *Proceedings of the CBPF International Workshop on Relativistic Aspects of Nuclear Physics*, Rio de Janeiro, 1989, edited by T. Kodama *et al.* (World Scientific, Singapore, 1990), p. 127.

⁸G. Baur and L. G. Ferreira Falho, Jülich report, 1990 (unpublished).

⁹E. Papageorgiu, *Phys. Lett. B* (to be published).

¹⁰J. S. Wu *et al.*, Oak Ridge National Laboratory Report No.

- ORNL/CCIP/90/02 (unpublished).
- ¹¹J. W. Norbury, this issue, *Phys. Rev. D* **42**, 3696 (1990).
- ¹²B. Müller and A. J. Schramm, this issue, *Phys. Rev. D* **42**, 3699 (1990).
- ¹³J. D. Jackson, *Classical Electrodynamics*, 2nd ed. (Wiley, New York, 1975), p. 722.
- ¹⁴H. Überall, *Electron Scattering from Complex Nuclei* (Academic, New York, 1971), Pt. A, Table IX, p. 210-1.
- ¹⁵J. Ellis, M. K. Gaillard, and D. Nanopoulos, *Nucl. Phys.* **B106**, 292 (1976).
- ¹⁶G. Altarelli and M. Traseira, *Phys. Lett. B* **245**, 658 (1990).